

Rugged Early-Warning Spectroscopic System for Real-Time Environment Water Monitoring

Bo Ling^{*a}, Michael I. Zeifman^b, Jannias Hu^a

^aMigma Systems Inc., 1600 Providence Hwy, Walpole, MA 02081

ABSTRACT

The absorption spectra of BWA/CWA often heavily overlap with each other and with absorption spectra of harmless species. The traditional approach of spectral discrimination usually involves estimation of concentration of each constituent, wherein the first- and second derivatives are being used as the spectrum features and the linear relationship between these features and the concentrations is sought by, e.g., the partial least squares or principal component regression. These algorithms may not be suitable for real-time early warning detection of BWA/CWA in the gaseous/liquid environments, especially taking into account the inevitable presence of environmental constituents with unknown spectra. In this paper, we present a new approach suitable for rugged, real-time spectral discrimination. In this approach, we are using an independent component analysis (ICA) technique to unmix the mixture spectra into independent spectral components. In order to classify the components, we have developed a special feature extraction algorithm based on a complex wavelet transform. We have tested the procedure experimentally using a rugged fiber-optics spectrometer working in the NIR region (800 – 1000 nm), and mixtures of organic liquids. The obtained results clearly demonstrate the applicability of the proposed system to the early warning “trigger”-type detection suitable for real-time environmental monitoring.

Keywords: independent component analysis, feature extraction, classification, NIR spectra

1. INTRODUCTION

Recent advances in chemical- and biotechnology, the low cost and ease of producing potent pathogens and dangerous chemicals as well as their relative invisibility have increased the likelihood for biowarfare (BW) and chemical warfare (CW) [1]. The ability to detect the release of a BW/CW agent before the onset of symptoms in exposed subjects can prevent numerous human and animal losses [2]. There is heightened awareness worldwide of the possibility of attacks on metropolitan areas using chemical and biological warfare agents (CWA/BWA) in waterways. A possible scenario of dissemination of BWA/CWA can be the spreading of the agents throughout the water intake or in a public beach area [3]. Depending on the specific agent used, the low solubilities of these agents may allow contaminants to persist for a long period, effectively functioning as a time-release system in moving from an insoluble state to the aqueous environment [4]. A large volume of the released agent may remain effective for years if the contaminated water body is static or slowly moving [4]. Some of these agents can also survive the standard water purification methods [5], thus compromising the security of drinking water reservoirs.

The most practical methods of BWA detection can be divided into three categories [1]: (i) immunological methods that are based on the use of antibodies [6], (ii) molecular biological techniques, e.g., in-situ hybridization [7] or polymerase chain reaction (PCR) [8] and (iii) spectroscopic methods. The biological sensors based on the first two detection methods are, e.g., optical sensors [9], [10] and electrochemical sensors [5]. These sensors, though very sensitive to minute concentrations of BWA, are deemed to be unsuitable for the rugged use in harsh environments [1]. The use of biological sensors based on the spectroscopic techniques is currently hindered by the low discrimination ability of such

* bling@migasys.com; phone 1 508 660-0328; fax 1 508 660-0288; www.migasys.com

sensors. While the vibrational (infrared) spectra of distinct biological species are clearly different, it is difficult to deconvolute the BWA signal in an IR spectrum of a mixture [1], [11], [12].

The vast variety of chemical agents has led to mostly agent-specific detection methods such as analytical methods [4]. Other major tools for CWA detection include liquid chromatography and mass spectrometry [13], Raman spectroscopy [14], microwave spectroscopy [15], photoacoustic spectroscopy [16], and laser-induced break-down spectroscopy [17]. The latter spectroscopic methods are prone to the same problem as the IR spectroscopy of BWA, the mathematical problem of unmixing/deconvoluting of a signal from the mixture. In this paper, we mainly concentrate on mathematical techniques of spectrum processing in the near-infrared region.

Near-infrared spectroscopy is an optical technique that involves measurements between the visible and the mid-IR region of the electromagnetic spectrum. Due to the fundamental nature of the absorption chemistry, information regarding almost all constituents of a sample is included in its spectral data [18]. Because the absorptions are secondary in nature, they are relatively weak (100–1000 times less than that in mid-IR), enabling direct analysis on samples with little or no sample preparation [19]. Moreover, the instrumentation for NIR spectroscopy is significantly less expensive than its MIR counterpart, especially in the 800-1100 nm region, where a CCD grating spectrometer can be used for spectrum acquisition.

Although spectral response in NIR spectroscopy may occasionally have a clearly assignable chemical basis, in practice the bands observed are broad, with severe overlaps and poor baseline resolution, making spectral interpretation difficult. A typical analyte would absorb at more than one wavelength and absorbance at a given wavelength may have contributions from more than one analyte. The physics governing the absorbance process is usually loosely described by the Beer-Lambert Law (or Beer's Law) which states that for an absorbing compound dissolved in a nonabsorbing medium, the concentration c of the compound is proportional to the absorbance (a)

$$c \propto a = \log_{10}(I_0 / I) \quad (1)$$

where I_0 is the light intensity incident on the medium and I is the light intensity transmitted through the medium. For a medium containing several different absorbing compounds (except at very high concentrations) the overall absorbance a is simply the sum of the contributions of each compound.

In eq. (1), the light intensities are wavelength-dependent so that a one-dimensional array or *spectrum* is available upon a single spectroscopic measurement. If several absorbing compounds are present in the medium, then the resulting absorbance (or transmittance) spectrum will be a linear mixture of the spectra of the individual components. The array size, i.e., the number of different wavelengths, is usually much larger than the number of components, so that the problem of the unmixing of a single spectrum can, in principle, be solved by a multivariate statistical technique, such as Least Squares, Partial Least Squares, Principal Component Regression and others. All these techniques require an extensive calibration stage, or *statistical training*, in terms of pattern recognition, and they usually do not tolerate the presence of an unknown species. Such an unknown species, having a distinct spectrum, cannot be treated as a Gaussian random noise, thus decreasing the statistical performance. Moreover, since this species was not included into the calibration stage, its concentration cannot be estimated, or, which is the same, the mere presence of an unknown species cannot be verified.

There are situations, however, in which it is not necessary to simultaneously determine the species presence and its concentration, but merely to detect the presence of a new species and classify it on the basis of, e.g., a spectral library, acquired elsewhere. In this case, other statistical techniques could be used instead of the concentration-based least squares and its variants. In this paper, we describe a system based on the concept of the independent component analysis (ICA). The system includes a CCD-based grating spectrometer, a standard flow cell, and an originally developed processing unit, which allows for near real-time liquid monitoring.

In the next section, we explain the basics of ICA as well as the improvements we made to accommodate the ICA for our purposes. The major improvement is the way of exploiting the internal structure of a spectrum to enhance the algorithm stability.

Proper signal processing implies the use of signal features rather than raw signals, because well-chosen features would be robust to signal fluctuations and also reduce the dimensionality of the problem. Moreover, the signals decomposed by ICA usually distorted as compared to the originals so that the features must be robust to such distortions. In Section 3, we present our features based on a complex wavelet transform.

The integrated system is described and a practical example based on the NIR spectra of water and two organic components is given in Section 4. It is shown that our system is capable of detection of a new component with a very low relative spectral abundance, of the order of 10^{-5} . Moreover, since the developed mathematical methodology does not depend on a specific spectral region, the system is generally applicable to UV, MIR spectra and to any acquisition method that implies a linear mixture.

2. INDEPENDENT COMPONENT ANALYSIS

2.1 ICA Basics

The independent component analysis (ICA) is a newly developed statistical approach to separating unobserved, independent source variables from the observed variables that are the combinations (or mixtures) of these source variables. Since it was developed in the 1990s (see [20], [21], [22]). ICA has proved to be a successful technique in biomedical signal processing [23], magnetic resonance imaging analysis [24], speech recognition [25] and machine monitoring [26].

Using the standard ICA methodology, we can write

$$\mathbf{X} = \mathbf{A} \cdot \mathbf{S} \quad (2)$$

where \mathbf{X} is a column matrix of mixed signals, \mathbf{A} is a matrix representing the signal abundances and \mathbf{S} is the column matrix of the source signals. With relation to the spectroscopic signals (viz. spectra), eq. (2) represents both Beer-Lambert law and the principle of superposition.

Because of the linearity of eq. (2), the inverse equation is also linear:

$$\mathbf{S} = \mathbf{A}^{-1} \cdot \mathbf{X} = \mathbf{B} \cdot \mathbf{X} \quad (3)$$

The key idea of ICA method is that thanks to the Central Limit Theorem, a weighted sum of column vectors of \mathbf{X} (eq. 3) tends to a normal (Gaussian) distribution unless it accidentally equals one of vectors of matrix \mathbf{S} . Therefore, by multiplying different matrices by the signal matrix and by measuring the degree of gaussianity of their product, the independent components can be detected. Of course, this formulation can only help find the “form” of the independent components, as scaling the matrix \mathbf{B} will also scale the solution, while the degree of non-gaussianity would not change.

ICA usually starts from a pre-procedure of “whitening”. The key idea here is that if the signals are independent, then they are uncorrelated, which in turn means that a procedure that decorrelates matrix \mathbf{X} is a necessary (but not sufficient) procedure for obtaining independent signals. The two-stage procedure will be maximally efficient if we also require unit variances of the decorrelated components, because, in this case, the meaning of the matrix \mathbf{B} will be the rotation of the “whitened” matrix \mathbf{X} . That is, ICA is usually performed in two stages:

- 1) $\mathbf{Z} = \mathbf{\Omega X}$
- 2) $\mathbf{W} : \mathbf{W} \cdot \mathbf{Z} \rightarrow \max(\text{non} - \text{Gauss})$

The matrix \mathbf{W} in this case is an orthonormal matrix which can be indeed considered as a rotation matrix in the n -dimensional space. Various degrees of non-gaussianity have been proposed so far, for example an estimated kurtosis or entropy can be used. Since for a normal distribution both kurtosis and entropy are minimal among all possible distributions for the whitened signals, their maximization will yield maximum of non-gaussianity. As for the first transform, it is just a well-known transform in principal component analysis (PCA) so that the matrix $\mathbf{\Omega}$ can be easily calculated on the basis of covariance matrix of \mathbf{X} . Being a high-order statistical technique, ICA outperforms the second-order PCA in the discrimination power [20-26].

2.2 Practical Implementation of ICA for Spectra Unmixing

As it follows from the previous sub-section, the use of ICA requires an input matrix which is a two-dimensional array, whereas a single spectrum is a one-dimensional array. Moreover, the internal structure of ICA implies that different rows in the input mixture matrix \mathbf{X}^T be spectra comprised of components at different concentrations (viz. spectral

abundances), as the ICA solution would not converge otherwise. This problem could be solved if the input matrix were composed of the spectra acquired at essentially different times so that the contribution of each individual component to the total mixture spectrum would likely change.

The optimization-based algorithms for ICA use random initial matrix. Such randomness may also lead to poor convergence and/or to the solution based on the local and not global maximum. To further improve the ICA performance, we implemented a specially developed procedure. The motivation is that the traditional ICA is not sensitive to the order of variables comprising a mixture vector. In other words, a random permutation of the obtained spectrum will not influence the conventional ICA in any way. To account for the signal structure, we first perform “temporal” ICA and then use the obtained unmixed matrix as the initial matrix for the conventional ICA algorithm.

The key idea behind “temporal” ICA is to exploit the internal structure of the mixed signals. In our case, it is wavelength structure of the spectra, but in traditional signal processing it is a time structure of a signal. The term “temporal” ICA is therefore due to this time structure.

The simplest form of time structure is given by autocovariances. This means, in relation to our problem, covariances between the values of the signal at different waveband points: $\text{cov} [\mathbf{x}_i(\lambda), \mathbf{x}_i(\lambda-\Delta)]$, where Δ is the waveband lag. The value of $\Delta = 1$ corresponds to the covariance between two adjacent points in the spectrum. In addition to the covariances within a single spectrum, we also need covariances between two signals: $\text{cov}[\mathbf{x}_i(\lambda), \mathbf{x}_j(\lambda-\Delta)]$. These statistics can be combined in the lagged covariance matrix

$$\mathbf{C}_{\Delta}^x = E[\mathbf{x}(\lambda)\mathbf{x}(\lambda - \Delta)^T] \quad (4)$$

In eq. (4), E designates the statistical expectation.

For the independent components, the lagged covariance matrix is a diagonal matrix because of the component independence. We should, therefore, seek for such matrix \mathbf{B} that the lagged covariance matrix of $\mathbf{Y} = \mathbf{B}\mathbf{X}$ is diagonal.

Let us assume that the data matrix \mathbf{X} has been whitened so that the resulting matrix \mathbf{Z} contains non-correlated vectors (spectra) with unit variances. Since the lagged covariance matrix eq. (4) is estimated by the experimental data, the matrix may not be exactly symmetric (the delay to the left may slightly differ from the delay to the right), although the true matrix is symmetric. To remedy this problem we consider

$$\overline{\mathbf{C}}_{\Delta}^z = \frac{1}{2}[\mathbf{C}_{\Delta}^z + (\mathbf{C}_{\Delta}^z)^T] \quad (5)$$

Using standard matrix operations, it can be shown that the sought concentration matrix \mathbf{W} is part of the eigenvalue decomposition of the estimable matrix $\overline{\mathbf{C}}_{\Delta}^z$ [21], since

$$\overline{\mathbf{C}}_{\Delta}^z = \frac{1}{2} \mathbf{W}^T \left\{ E[\mathbf{s}(\lambda)\mathbf{s}(\lambda - \Delta)^T] + E[\mathbf{s}(\lambda - \Delta)\mathbf{s}(\lambda)^T] \right\} \mathbf{W} = \mathbf{W}^T \overline{\mathbf{C}}_{\Delta}^s \mathbf{W} \quad (6)$$

The obtained matrix \mathbf{W} is then being used as the initial matrix in a standard fast ICA algorithm [21].

The last important practical question related to ICA implementation is related to the number of components. Eqs. (2)-(5) imply that the number of components equal to the number of source vectors in matrix \mathbf{X} . In reality, the number of components is significantly less, and in application to the water monitoring problem, the number of significant components could be as small as two or three.

In our algorithm, the most significant components are calculated automatically on the basis of the eigenvalue structure. Fig. 1 illustrates the key idea. The eigenvalues are logarithmed and sorted, and the mean and standard deviation of the smallest 50% of eigenvalues are calculated as well as the mean difference between two adjacent small eigenvalues and its standard deviation. The algorithm firstly seeks when the difference between the eigenvalues becomes small in comparison with the calculated measures. Since there might be large eigenvalues with a very small difference between them, the algorithm then looks for eigenvalues that are significantly larger than the remaining eigenvalues.

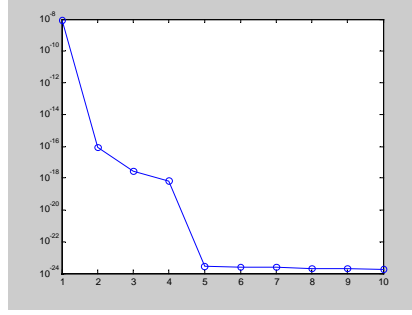


Fig. 1. Typical eigenvalues of the covariance matrix of mixed spectra.

3. SPECTRAL FEATURES

To make the procedure of spectrum classification and identification feasible, meaningful spectral features should be used instead of the raw spectra. We propose to use wavelet transform to identify such features.

Let $x(t)$ be the spectral signal. The complex wavelet transform, using a well-chosen complex wavelet $\psi(t)$ with scale parameter s (setting the frequency range) and translation parameter t (determining the time localization), is defined as [27]

$$f_W(t, s) = \int_{-\infty}^{+\infty} f(\tau) \frac{1}{\sqrt{s}} \Psi\left(\frac{\tau-t}{s}\right) d\tau \quad (7)$$

In a single-phase system this yields two series of complex wavelet coefficients for $x(t)$, $X_W(t, s)$:

$$X_W(t, s) = A_W(t, s) e^{j\varphi_W(t, s)} \quad (8)$$

where $A_W(t, s)$ is the absolute value of $X_W(t, s)$ and $\varphi_W(t, s)$ is the phase. Here we propose to use the complex Gaussian wavelet

$$\Psi_G(t) = c_p e^{-t^2} e^{-jt} \quad (9)$$

where c_p is the scaling parameter, f_b is the bandwidth parameter and f_c the center frequency.

Fig. 2 shows the wavelet features as applied to a library spectrum of H_2S from HITRAN data base [28] along with the standard Fourier features. It is seen in the figure that the wavelet features have a distinct characteristic shape. They are also robust to the ICA-induced distortions and noise. Depending on the application, i.e., on the geometrical shape of the original spectrum, the mathematical utilization of the features can be different. As applied to the relatively smooth spectra of water and biological agents, we use the averages and standard deviations of the real and imaginary parts of the wavelet features (see Section 4.2 for details).

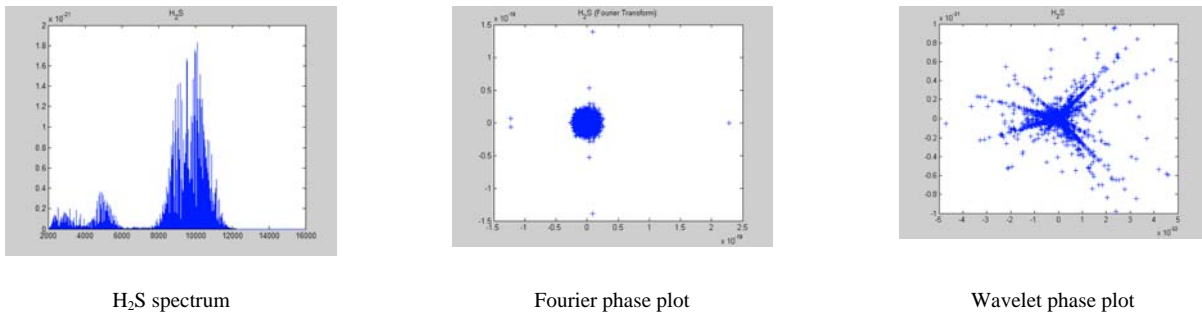


Fig. 2. A library spectrum of H_2S from HITRAN database and its Fourier and wavelet features.

4. REAL-TIME SYSTEM

4.1 Schematic Description

Our system consists of two major blocks, the data acquisition unit and the data processing unit. The data acquisition unit comprises a grating CCD spectrophotometer and a standard flow cell. Both parts are COTS units and therefore are not shown here. The data processing unit is originally developed by our company, Migma Systems, Inc.

Fig. 3 shows a schematic of the data processing unit. A spectrum acquired by the data acquisition unit enters the ICA input matrix block. As the new spectrum enters, the oldest real-time spectrum (#70 in terms of Fig. 3) leaves the block. Certain part of the matrix is reserved for the pre-acquired spectra to maintain algorithm convergence.

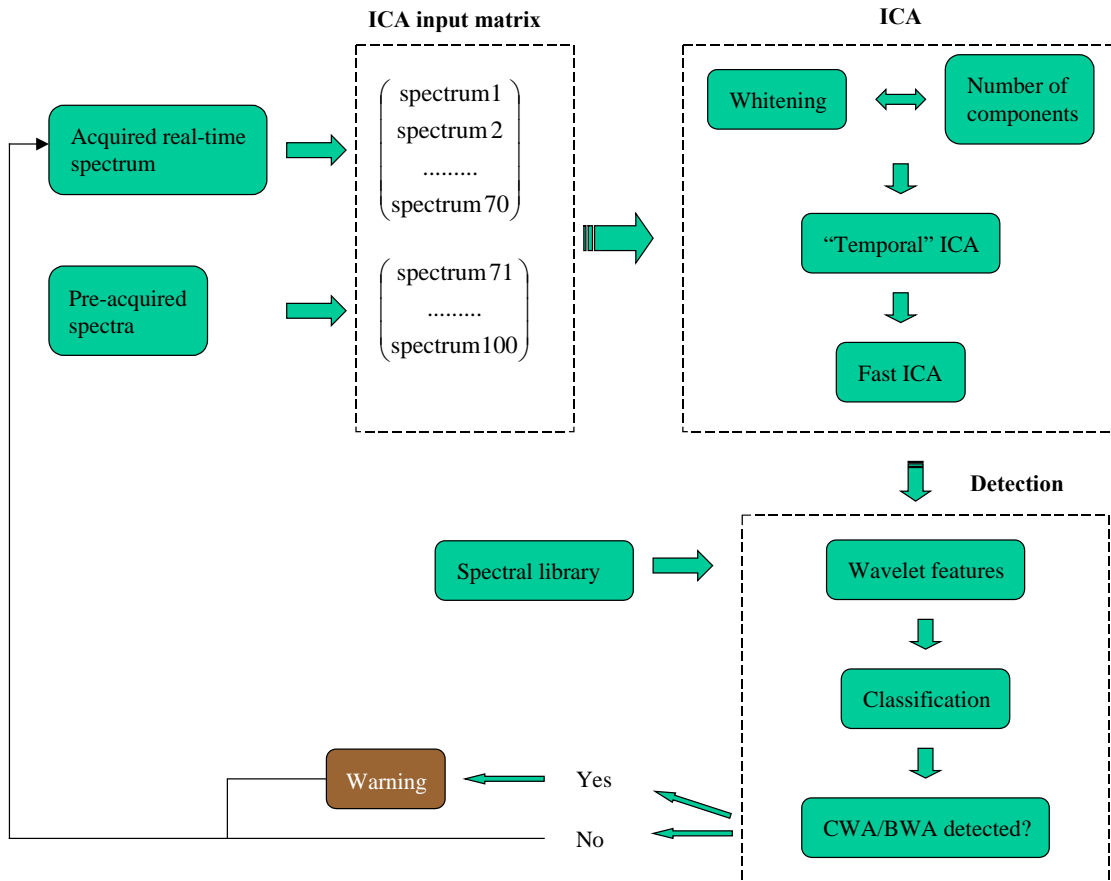


Fig. 3. Schematic of the data processing unit.

The compiled matrix enters the ICA block where it is whitened and the number of significant components is determined. The initial unmixed matrix is then determined by the “temporal” ICA and is used as the initial value in a fast ICA algorithm.

The decomposed signals then enter the detection block where their features are being compared with the features calculated for the desired spectra from a library. If an CWA/BWA is detected, the warning alert is issued and the system proceeds with the next real-time spectrum.

Our system was originally written in MATLAB and then ported to C/C++ with a GUI implementation on a Windows machine. It is capable of processing approximately 2 spectra/second.

4.2 Practical Example

The main advantages of our system are (i) the use of a rugged inexpensive CCD grating spectrometer for data acquisition, and (ii) a new methodology for data processing. Depending on the application and correspondingly on the spectral region of interest, e.g., UV, NIR, MIR, the data acquisition system can be changed. The mathematical methodology, however, will remain the same. In this sub-section, we illustrate the methodology on an example from biological process monitoring.

Fig. 4 shows the second derivative transmittance spectra of three species chosen as a representative simulation system for BWA detection. Water and ammonium are chosen as basic species that are supposed to be always present. Glucose is chosen as a simulant of a BWA/CWA. The reason of choosing glucose is that its aqueous solution spectrum is close to the water spectrum so that the conventional methods of signal separation, like PCA, will fail in detection of this species.

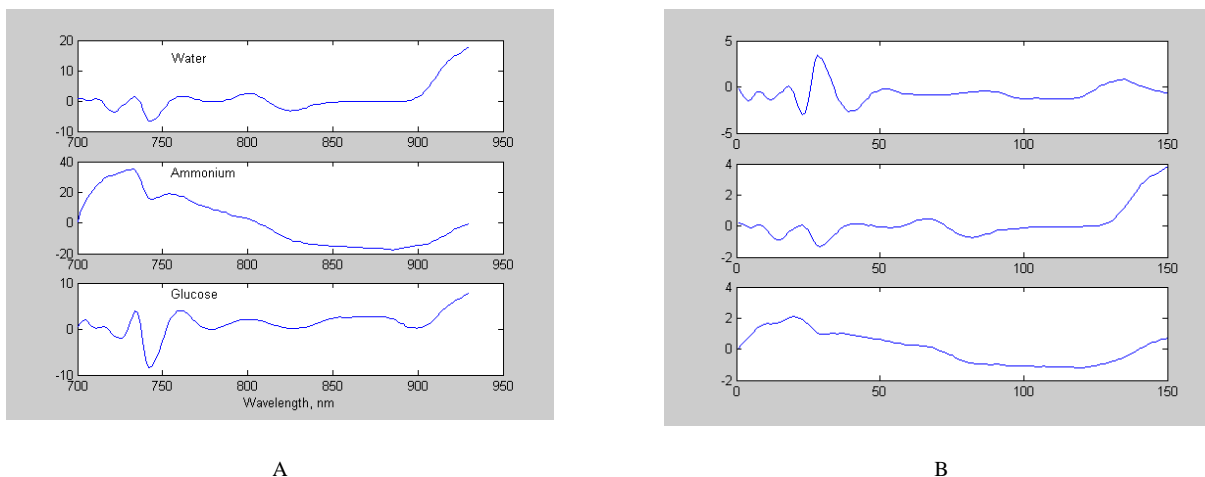


Fig. 4. A: The second derivative transmittance spectra of water and aqueous solutions of ammonium and glucose. Glucose is used as a BWA/CWA simulant. B: The decomposed components. Note that some of components are upward down as compared to the originals.

In order to demonstrate the system, we created a mixed matrix **A** from these three components, taking the target weight (“concentration” or spectral abundance) of water spectrum in the mixture being about 75% and the target weight of a glucose solution spectrum being 1%, 0.1% and 0.001%. Each row of matrix **A** was composed as a mixture of the three components taken with weights randomly fluctuated around the target value. Fig. 4(B) shows the typical decomposed signals. It is seen in the figure that even though the decomposed signals are close to the originals, they are distorted in shape.

This distortion as well as the noise necessitates the use of features. Fig. 5 shows the wavelet phase plots of the decomposed signal. Interestingly, even though the components 1 and 2 are close in shape, their phase plots are very different. Based on these preliminary data, we have chosen the averages and standard deviations of the real and imaginary parts of the wavelet transform, which reduced the dimension of the original spectrum (150 data points) to just four in the feature space.

In order to test the features, we have run the simulations with different spectral abundances of the BWA simulant (glucose) and with addition of a Gaussian noise. The noise was added in such a way that its standard deviation equals to four standard deviations of the glucose signals. 100 repetitions were made for each spectral abundance. The obtained results for the spectral abundances of 10^{-3} and 10^{-5} of the BWA simulant are shown in Fig. 6 as well as the features

obtained on the basis of the original second-derivative spectra. It is seen in the figure that the chosen features allow for good signal separation as no overlap has occurred between the features of different signals. A simple distance classifier can then separate and classify the unmixed signals on the basis of these features.

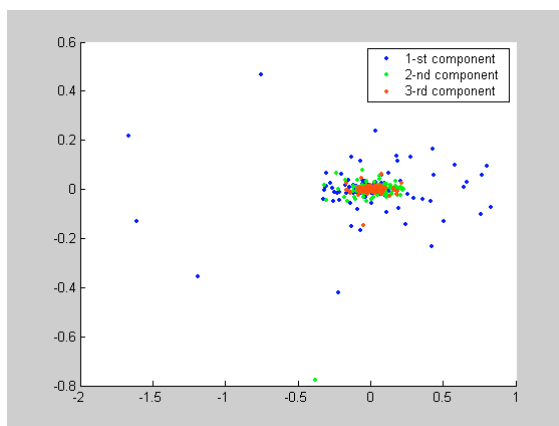


Fig. 5. Complex wavelet phase plot of the decomposed signals shown in Fig. 4.

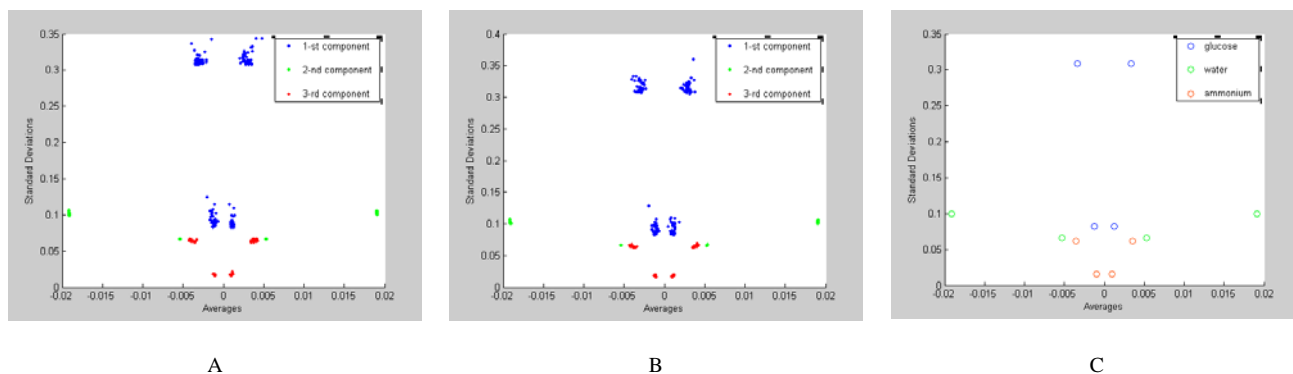


Fig. 6. The results of 100 simulation runs in the feature space (average and standard deviation of real/imaginary parts of complex wavelet transform). The target spectral abundance of water is about 75%, the abundance of ammonium is approximately 25% and the abundance of glucose (BWA simulant) is 0.1% (A) and 0.001% (B). The features of the original second-derivative spectra are shown also (C).

5. CONCLUSION

In this paper, we have presented an innovative system for near real-time monitoring of water for the presence of BWA/CWA. The spectral absorbance in the NIR region is used for signal decomposition based on the independent component analysis instead of traditional concentration-based methods. Complex wavelet transform based features applied to the decomposed signal enable reliable detection and classification of a trace species provided that its spectrum is approximately known. Because the system can easily be adapted to any spectrometer, it is a viable choice of BWA/CWA detection and other commercial applications.

Acknowledgement: This work is supported by US Army under Contract: W911NF-04-C-0099.

REFERENCES

1. L.A. Vanderberg, "Detection of biological agents: looking for bugs in all the wrong places," *Applied Spectroscopy*, 54, 376A-385A (2000).

2. L.D. Rotz and J.M. Hughes, "Advances in detecting and responding to threats from bioterrorism and emerging infectious disease," *Nature Medicine* 10, S130-S136 (2004).
3. H.C. Lane, J.L. Montagne, A.S. Fauci, "Bioterrorism: a clear and present danger," *Nature Medicine* 7, 1271-1273 (2001).
4. H.B. Glasgow, J.M. Burkholder, R.E. Reed, A.J. Lewitus, J.E. Kleinman, "Real-time remote monitoring of water quality: a review of current applications, and advancements in sensor, telemetry, and computing technologies," *Journal of Experimental Marine Biology and Ecology* 300 (1-2): 409-448 (2004).
5. J. Shah, E. Wilkins. Electrochemical Biosensors for Detection of Biological Warfare Agents. *Electroanalysis* 15, 157-167 (2003).
6. J. J. Perry and J. T. Staley. *Microbiology: Dynamics and Diversity*. Saunders College Publishing, Forth Worth, Texas (1997).
7. R.A. Keller, W.P. Ambrose, P.M. Goodwin, J.H. Jett, J.C. Martin, M. Wu. Single molecule fluorescence analysis in solution. *Applied Spectroscopy* 50, A12-A32 (1996).
8. D. Ivnitski, D.J. O'Neil, A. Gattuso, R. Schlicht, M. Calidonna, R. Fisher. Nucleic acid approaches for detection and identification of biological warfare and infectious disease agents. *Biotechniques* 35, 862-869 (2003).
9. A.N. Naimushin, C.B. Spinelli, S.D. Soelberg, T. Manna, R.C. Stevens, T. Chinowsky, P. Kauffman, S. Yee, C.E. Furlong, "Airborne analyte detection with an aircraft-adapted surface plasmon resonance sensor system," *Sensors and Actuators B* 104, 237-248 (2005).
10. E.A. Perkins and D.J. Squirrell. "Development of instrumentation to allow the detection of microorganisms using light scattering in combination with surface plasmon resonance." *Biosensors & Bioelectronics* 14, 853-859 (2000).
11. D. Naumann, V. Fijala, H. Labischinski, P. Giesbrecht. "The Rapid Differentiation and Identification of Pathogenic Bacteria Using Fourier-Transform Infrared Spectroscopic and Multivariate Statistical-Analysis." *Journal of Molecular Structure* 174, 165-170 (1988).
12. Z. Filip, S. Herrmann, J. Kubat. "FT-IR spectroscopic characteristics of differently cultivated *Bacillus subtilis*." *Microbiological Research* 159, 257-262 (2004).
13. R.M. Black, B. Muir "Derivatisation reactions in the chromatographic analysis of chemical warfare agents and their degradation products," *Journal of Chromatography A* 1000 (1-2): 253-281 (2003).
14. D.A. Stuart, K.B. Biggs, R.P. Van Duyne, "Surface-enhanced Raman spectroscopy of half-mustard agent," *Analyst* 131 (4): 568-572 (2006).
15. R.R. Bousquet, P.M. Chu, R.S. DaBell, et al., "Trends in microwave spectroscopy for the detection of chemical agents," *IEEE Sensors Journal* 5 (4): 656-664 (2005).
16. M.E. Webber, M. Pushkarsky, C.K.N. Patel, "Optical detection of chemical warfare agents and toxic industrial chemicals: Simulation," *Journal of Applied Physics* 97 (11): Art. No. 113101 (2005).
17. F.C. DeLucia, A.C. Samuels, R.S. Harmon, et al., "Laser-induced breakdown spectroscopy (LIBS): A promising versatile chemical sensor technology for hazardous material detection," *IEEE Sensors Journal* 5 (4): 681-689 (2005).
18. E.W. Ciurczak.. In: Burns DA, Ciurczak EW, editors. *Handbook of near-infrared analysis*. New York: Marcel Decker Inc. p. 13-17 (1992).
19. J. Workman. "A closer look at NIR measurements." *NIR News* 7(2): 8-9 (1996).
20. P. Comon, "Independent Component Analysis - a New Concept?" *Signal Processing* 36, 287-314 (1994).
21. A. Hyvarinen, "Survey on Independent Component Analysis," *Neural Computing Surveys*, 2, 94-128 (1999).
22. C. Jutten, H. Herault, "Blind Separation of Sources, Part I: an Adaptive Algorithm Based on Neuromimetic Architecture," *Signal Processing*, 23, 1-10 (1991).
23. R.N. Vigario, "Extraction of Ocular Artifacts from EEG using Independent Component Analysis," *Electroencephalograph. Clin. Neurophysiol.*, 103, 395-404 (1997).
24. B.B. Biswal, J.L. Ulmer, "Blind Source Separation of Multiple Signal Sources of MRI Data Sets Using Independent Component Analysis," *J. Comput. Assist. Tomogr.*, 23, 265-271 (1999).
25. H. M. Park, H.Y Jung, T.W. Lee, S.Y. Lee, "Subband-based Blind Signal Separation for Noisy Speech Recognition," *Electronics Lett.*, 35, 2011-2012 (1999).
26. A. Ypma, P. Pajunen "Rotating Machine Vibration Analysis with Second-order Independent Component Analysis," Proc. Workshop on Independent Component Analysis and Signal Separation (ICA99); Aussois, France, pp 37-42. (1999).
27. S. Mallat, *A Wavelet Tour of Signal Processing*, Academic Press (1999).
28. <http://cfa-www.harvard.edu/HITRAN>